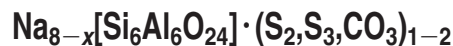


## Synthesis and Characterization of the Ultramarine-Type Analog



Esteban Climent-Pascual,<sup>†</sup> Julio Romero de Paz,<sup>‡</sup> Juan Rodríguez-Carvajal,<sup>§</sup> Emmanuelle Suard,<sup>§</sup> and Regino Sáez-Puche<sup>\*†</sup>

<sup>†</sup>Departamento de Química Inorgánica I, Facultad Ciencias Químicas, Universidad Complutense Madrid, E28040 Madrid, Spain, <sup>‡</sup>CAI Técnicas Físicas, Facultad Ciencias Físicas, Universidad Complutense Madrid, E28040 Madrid, Spain, and <sup>§</sup>Institut Laue-Langevin, BP 1566, 38042 Grenoble Cedex 9, France

Received March 5, 2009

The use of nitrite sodalite as a precursor to prepare new blue ultramarine analogs has been investigated. The encapsulation of the chromophores inside of  $\beta$  cages was achieved by heating the nitrite sodalite precursor with a mixture of sodium carbonate, sulfur, and a reducing agent at about 1000 K under airtight conditions. The obtained new blue ultramarine-type material was characterized by means of X-ray and neutron powder diffraction, transmission electron microscopy, <sup>29</sup>Si magic-angle-spinning NMR, IR, Raman, and diffuse reflectance spectroscopies. Thermogravimetric analysis and magnetic measurements were performed in order to determine water and chromophore contents, respectively. On the basis of the spectroscopic results and Rietveld analysis of neutron powder data, the  $\beta$  cage filling was found to be yellow  $\text{S}_2^-$  and blue  $\text{S}_3^-$  chromophores along with carbonate anions. The determined chromophore concentration, about 0.31 mol per formula unit, is enough to have greenish-blue ultramarines, which proves that ultramarine analogs can be obtained from nitrite sodalite.

### Introduction

Ultramarine pigments are aluminosilicates of sodalite structure with sulfur chromophore species entrapped within the so-called  $\beta$  cages.<sup>1–3</sup> The naturally occurring ultramarine (lazarite) only has a deep blue color, while synthetic ones are commercially available in green, blue, violet, and pink. The color of the blue ultramarine is due to the  $\text{S}_3^-$  chromophores, which are oligosulfide anion radicals.<sup>4–9</sup> These chromophores are located near the center of the  $\beta$  cage in a 4-fold tetrahedral coordination with sodium cations. These extra-framework cations are inserted to neutralize the deficit of positive charges induced by the presence of aluminum atoms

in the zeolitic framework and chromophores inside of the  $\beta$  cages,<sup>10,11</sup> see Figure 1. Besides the blue chromophore, representing the majority of blue ultramarine chromophores, a minor proportion of yellow  $\text{S}_2^-$  and red  $\text{S}_4^-$  and  $\text{S}_4$  chromophores has been also identified.<sup>6,12,13</sup> However, not all  $\beta$  cages are occupied by chromophores since some of them are filled by other anionic species such as chloride and sulfate anions or are not even filled with anions at all.<sup>2,3,14</sup> This variety of  $\beta$  cage filling is structurally possible because of the high flexibility of the sodalite-type structure through cooperative rotation of the framework tetrahedra, allowing it to adjust to the size of the species entrapped within the  $\beta$  cages.<sup>2</sup> Concerning this latter aspect, framework cations and their ratio are limiting factors in the adaptation capacity of the sodalitic framework. The naturally occurring lazurite has a  $\text{Si}^{4+}/\text{Al}^{3+}$  ratio equal to unity, and the framework cations are distributed in an orderly manner. However, in synthetic ultramarine pigments, obtained at high temperatures by a ceramic method, this ratio is higher than unity, and the cations are randomly distributed.<sup>11,15</sup> Therefore, synthetic ultramarine pigments have the general

\*To whom correspondence should be addressed. Tel.: +34 91 394 4353. Fax: +34 91 394 4352. E-mail: rsp92@quim.ucm.es.

(1) Buxbaum, G.; Pfaff, G. *Industrial Inorganic Pigments*; Wiley-VCH: Weinheim, Germany, 2005.

(2) Hassan, I.; Grundy, H. D. *Acta Crystallogr.* **1984**, *B40*, 6.

(3) Weller, M. T. *J. Chem. Soc., Dalton Trans.* **2000**, 4227.

(4) McLaughlan, S. D.; Marshall, D. J. *J. Phys. Chem.* **1970**, *74*, 1359.

(5) Clark, R. J. H.; Franks, M. L. *Chem. Phys. Lett.* **1975**, *34*, 69.

(6) Clark, R. J. H.; Cobbold, D. G. *Inorg. Chem.* **1978**, *17*, 3169.

(7) Clark, R. J. H.; Dines, T. J.; Kurmoo, M. *Inorg. Chem.* **1983**, *22*, 2766.

(8) Reinen, D.; Lindner, G.-G. *Chem. Soc. Rev.* **1999**, *28*, 75.

(9) Arieli, D.; Vaughan, D. E. W.; Goldfarb, D. *J. Am. Chem. Soc.* **2004**, *126*, 5776.

(10) Gobeltz, N.; Demortier, A.; Lelieur, J. P.; Duhayon, C. *J. Chem. Soc., Faraday Trans.* **1998**, *94*, 2257.

(11) Tarling, S. E.; Barnes, P.; Klinowski, J. *Acta Crystallogr.* **1988**, *B44*, 128.

(12) Landman, A. A.; De Waal, D. *Cryst. Eng.* **2001**, *4*, 159.

(13) Fabian, J.; Komiha, N.; Lingerri, R.; Rosmus, P. *THEOCHEM* **2006**, *801*, 63.

(14) Climent-Pascual, E.; Sáez-Puche, R.; Gómez-Herrero, A.; Romero de Paz, J. *Microporous Mesoporous Mater.* **2008**, *116*, 344.

(15) Gordillo, M. C.; Herrero, C. P. *Chem. Phys. Lett.* **1992**, *200*, 424.

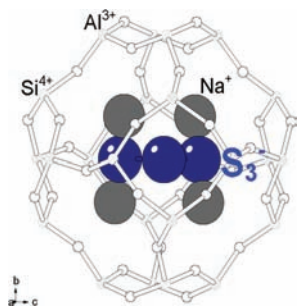


**Figure 1.** The blue chromophore  $S_3^{2-}$  trapped inside of a  $\beta$  cage.

formula:  $Na_{8-x}[(Si,Al)_{12}O_{24}] \cdot (S_2, S_3, S_4, SO_4, Cl)_{1-2}$ , which implies a theoretical maximum quantity of one chromophore per  $\beta$  cage.<sup>16</sup>

The synthesis of ultramarine-type materials has been widely studied since 1828 when Baptiste Guimet in France and Gottlob Gmelin in Germany independently succeeded in preparing a synthetic variety of blue ultramarine by heating a mixture of metakaolin (kaolin dehydroxylated at about 820 K), sulfur, sodium carbonate, and a reducing agent (coal, pitch, etc.).<sup>1</sup> Since then, blue ultramarine began to be industrially produced and used in a variety of applications. Nowadays, the industrial synthesis of blue ultramarine is conducted in two steps. The first consists of heating the mixture at about 1000 K under airtight conditions for a given period of time. The second step, performed after cooling down to about 720 K, is an oxidation under a sulfur dioxide environment. The sulfur dioxide arises from the reaction between the oxygen in the air and sulfur.<sup>1</sup> The search for new synthetic routes and color varieties continues even today. In this sense, natural and synthetic zeolites (Linde type A, faujasite, erionite, cancrinite, chabazite, stilbite, etc.), instead of the layered silicates (kaolin), have been investigated as potential starting materials of ultramarine analogs.<sup>17–19</sup> It has been suggested that these zeolitic precursors can be transformed into sodalite at about 1000 K with a high alkalinity mixture of sodium sulfide and sulfur, or sodium carbonate and sulfur (as source of oligosulfides), under airtight conditions. These conditions allow a collapse of the precursor structure and begin a recrystallization process. Here, the chromophores are simultaneously generated and trapped within the  $\beta$  cages of the sodalitic framework, just like the typical industrial synthesis mechanism. Ultramarine materials obtained in this way usually have a deep blue color. However, in some cases, if the temperature (700 K) and alkalinity are low, then the zeolitic precursor's structure remains and the chromophores diffuse with difficulty into zeolitic cages. Under these conditions, the colors obtained are pale blue or, in some cases, green. On the other hand, if the precursor is an already synthesized sodalite, then the chromophores can only diffuse into  $\beta$  cages at high temperatures because, under these conditions, their kinetic diameters are compatible with the dynamic opening of cage windows.<sup>10</sup> Blue ultramarine pigments have also been synthesized by

heating a previously obtained sodalite with aluminum sulfate and an organic template, tetramethylammonium hydroxide, at high temperature.<sup>9</sup> This latter synthesis method allows us to generate oligosulfide chromophores by intracage reduction of sulfate anions using the organic template as the source of reducing agents. Alternatively, ultramarines can be obtained from rhodanide sodalite by slow intracage oxidation of the thiocyanate anion in the air at high temperatures to yield sodalites containing oligosulfides.<sup>20–22</sup>

In this work, we present a new, simple synthetic route to prepare a blue ultramarine analog using as a precursor the nitrite sodalite  $Na_8[Al_6Si_6O_{24}](NO_2)_2$ . It is well-known that nitrite sodalites can serve as starting materials for the preparation of  $Na_8[Al_6Si_6O_{24}](NO_2)_{2-x}(NO_3)_x$ ,<sup>22,23</sup>  $Na_8[Al_6Si_6O_{24}]CO_3$ ,<sup>24,25</sup>  $(La, Nd)_4[Al_8Si_4O_{24}](WO_4)_2$ ,<sup>26</sup> and so forth. Thus, the thermally labile  $NO_2^-$  anion can be replaced by other anions at about 1000 K without any changes in the zeolitic framework. The present study then aims to investigate the encapsulation of chromophores inside of the  $\beta$  cages by heating nitrite sodalite with a mixture of sodium carbonate, sulfur, and a reducing agent. The new ultramarine-type material was characterized by X-ray powder diffraction, neutron powder diffraction, transmission electron microscopy, <sup>29</sup>Si magic-angle spinning nuclear magnetic resonance (<sup>29</sup>Si MAS NMR), IR, Raman, and diffuse reflectance spectroscopies. The total concentration of the paramagnetic anion radicals  $S_2^-$  and  $S_3^-$  was determined from magnetic susceptibility measurements.

## Experimental Section

**1. Synthesis.** Nitrite sodalite precursor  $Na_8[Al_6Si_6O_{24}](NO_2)_2$  was prepared by following a well-established hydrothermal synthetic route.<sup>25</sup> A reaction mixture of 1 g of kaolin (Riedel-de Haën), 25 mL of an 8 N NaOH (Panreac, PRS-CODEX) solution, and 0.7 g of sodium nitrite (Fluka, ACS reagent,  $\geq 99.0\%$ ) was transferred into a 50 mL Teflon-lined stainless steel autoclave and treated hydrothermally at 473 K for 24 h. After the reaction period, the clear basic solution was decanted, and the obtained white powder was washed with distilled water and dried at 353 K for 24 h.

The ultramarine-type material with nominal composition  $Na_8[Al_6Si_6O_{24}] \cdot (S_2, S_3)_2$  was synthesized as follows: A homogeneous mixture of 1 g of nitrite sodalite, 0.8 g of anhydrous sodium carbonate (Fluka, ultra,  $\geq 99.5\%$ ), 1 g of sulfur precipitate (Scharlau, extra pure), and 0.1 g of activated charcoal (SAJ, first grade) was heated gradually up to 973 K in a sealed alumina crucible and treated for 12 h. The obtained greenish-blue powder was washed with distilled water and dried at 353 K for 6 h.

**2. Characterization Techniques.** X-ray powder diffraction patterns were registered on a Philips Panalytical X'Pert MPD diffractometer (Cu  $K\alpha_1$ ,  $\lambda = 1.54056 \text{ \AA}$ ). Data were collected in the  $2\theta$  range between 5 and  $110^\circ$  in steps of  $0.017^\circ$ .

Neutron powder diffraction data were collected on high-resolution powder diffractometer D2B ( $\lambda = 1.594 \text{ \AA}$ ) at the Institute Laue-Langevin (Grenoble, France). Data were collected at 298 K

(16) Gobeltz-Hauteceour, N.; Demortier, A.; Lede, B.; Lelieur, J. P.; Duhayon, C. *Inorg. Chem.* **2002**, *41*, 2848.

(17) Kowalak, S.; Jankowska, A.; Łączkowska, S. *Catal. Today* **2004**, *90*, 167.

(18) Kowalak, S.; Jankowska, A. *Eur. J. Mineral.* **2005**, *17*, 861.

(19) Kowalak, S.; Jankowska, A. *Microporous Mesoporous Mater.* **2003**, *61*, 213.

(20) Hund, F. Z. *Anorg. Allg. Chem.* **1984**, *511*, 225.

(21) Buhl, J.-Ch.; Gesing, Th. M.; Gurrus, Ch. *Microporous Mesoporous Mater.* **2001**, *50*, 25.

(22) Weller, M. T.; Wong, G.; Adamson, C. L.; Dodd, S. M.; Roe, J. J. *J. Chem. Soc., Dalton Trans.* **1990**, 593.

(23) Buhl, J.-Ch. *J. Solid State Chem.* **1991**, *91*, 16.

(24) Buhl, J.-Ch. *J. Solid State Chem.* **1991**, *94*, 19.

(25) Gesing, T. M.; Buhl, J.-Ch. *Eur. J. Mineral.* **1998**, *10*, 71.

(26) Lezhnina, M.; Laeri, F.; Benmouhadi, L.; Kynast, U. *Adv. Mater.* **2006**, *18*, 280.

in the  $2\theta$  range between 6 and  $160^\circ$  in steps of  $0.05^\circ$  and analyzed by the Rietveld method using the FullProf program integrated in the WinPLOTR software.<sup>27</sup> Diffraction peaks were modeled using a pseudo-Voigt function convoluted with an axial divergence asymmetry function. The background was determined by means of a polynomial function.

Selected area electron diffraction (SAED) patterns were obtained on a JEM 2000FX microscope operated at 200 kV and equipped with a double-tilt specimen holder ( $\pm 45^\circ$ ). The sample was crushed in butanol using an agate mortar and pestle. It was then ultrasonically dispersed in butanol, and finally, the crystals in suspension were deposited on a holey carbon film supported on nickel grids.

Solid-state  $^{29}\text{Si}$  MAS NMR spectroscopy was performed using a Bruker MSL 400 spectrometer. The spectra were obtained at room temperature at 74.49 MHz. The samples were spun at 10 kHz, and a total of 1600 scans were accumulated. The excitation pulse and recycle time were  $6\ \mu\text{s}$  and 5 s, respectively. Tetramethylsilane was used as the external standard.

IR spectroscopy was carried out on a Nicolet IR200 FT-IR spectrometer in the range of  $4000\text{--}400\ \text{cm}^{-1}$ . The samples were hand-mixed with an agate mortar with KBr to obtain a pellet after compression on a dye.

Raman spectra were obtained at room temperature through the spinning sample technique using a Jobin-Yvon HR 460 monochromator. The excitation light was the 514.5 nm line of a Spectra Physics Ar–Kr laser. The incident and scattered beams were focused using an Olympus BX60 M microscope, and a Kaiser SuperNotchfilter was used to suppress the elastic light. The laser power was reduced down to 0.1 mW in order to avoid the local heating of the samples at the laser spot. The spectra were recorded between 50 and  $3000\ \text{cm}^{-1}$ , and the wavenumber shifts were calibrated using a silicon plate.

Magnetic susceptibility measurements were done using a Quantum Design XL-SQUID magnetometer in the temperature range between 1.9 and 200 K with a 0.5 T magnetic field.

Thermogravimetric analysis was performed on a Perkin-Elmer TGA Pyris 1 thermobalance under a pure oxygen flow. The measurement was carried out in the temperature range 298–1400 K with a heating rate of 10 K/min.

Colorimetric parameters were obtained on a Luci 100 colorimeter (viewing geometry  $d/8^\circ$ ,  $10^\circ$ -standard observer and D65 illuminant). In order to study the color of the blue analog, the Commission Internationale de l'Eclairage CIELAB 1976 space of colors, which uses three colorimetric parameters:  $L^*$ ,  $C^*$ , and  $h$ , was utilized. The first parameter, lightness, represents the ability of a sample to transmit or reflect a fraction of the incident light diffusely (0 for a black sample and 100 for a white sample). The second one, the so-called chroma, represents the amount of chromatic component or color purity (0 for the minimum amount and 100 for the highest). The final parameter, hue, represents the hue angle or colorimetric angle ( $0^\circ$  for a red color,  $90^\circ$  for a yellow color,  $180^\circ$  for a green color, and  $270^\circ$  for a blue color).<sup>28</sup> Moreover, the evaluation of the colorimetric parameters of the obtained analog was carried out with respect to a commercial reddish-blue ultramarine sample supplied by Nubiola Inorganic Pigments.

## Results and Discussion

The X-ray powder diffraction patterns for the precursor and the obtained blue ultramarine indicate pure phases with a sodalite-type structure, see Figure 2. If we suppose that the framework cations,  $\text{Al}^{3+}$  and  $\text{Si}^{4+}$ , are ordered, then, for

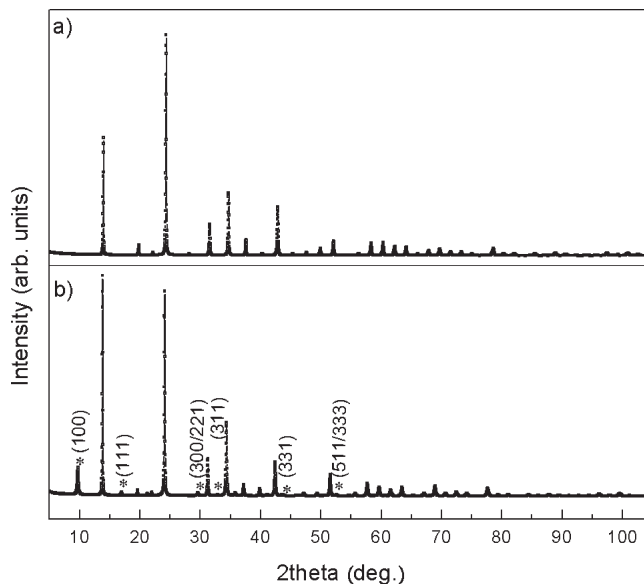


**Figure 2.** X-ray powder diffraction patterns of the nitrite sodalite precursor (a) and the obtained blue ultramarine-type analog (b). Asterisks indicate the onset of extra  $hhl$  with  $l = 2n + 1$  reflections.

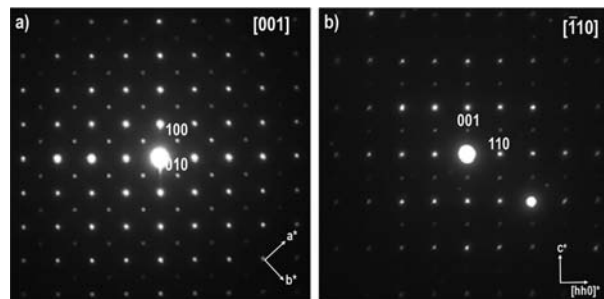


**Figure 3.** SAED patterns of the obtained blue ultramarine-type analog.

the nitrite sodalite precursor, all of the reflections may be indexed by the space group  $P\bar{4}3n$  (No. 218). However, for the obtained blue ultramarine-type analog, the onset of extra reflections, highlighting the 100 reflection, indicates  $\beta$  cage cluster ordering at the unit cell level, and therefore the suitable space group is  $P23$  (No. 195). Thus, a change from a sodalite-like to a nosean-like phase takes place.<sup>14,22</sup> Figure 3a shows the [001] SAED pattern for the obtained blue ultramarine analog. Besides the strong  $hhl$  with  $l = 2n$  reflections, weaker  $hhl$  with  $l = 2n + 1$  reflections are clearly seen as well, which confirms that the space group  $P23$  describes the structure of this new ultramarine-type material well. By tilting the crystal around the [110] direction, the corresponding  $[\bar{1}10]$  and [111] SAED patterns were obtained, see Figure 3b. As expected, they agree with the proposed space group. These observations show that, in the obtained blue ultramarine-type analog, the clusters located at the vertex and the center of the cubic unit cell are not equivalent, a fact that has been reported earlier in regard to other members of the sodalite family.<sup>29–32</sup>

Figure 4a and b show the solid-state  $^{29}\text{Si}$  MAS NMR spectra for the precursor and the obtained blue ultramarine-type

(27) Rodríguez-Carvajal, J.; Roisnel, T. FullProf, WinPLOTR, and accompanying programs, 2008. <http://www.ill.eu/sites/fullprof/index.html> (accessed June 2009).

(28) Nassau, K. *The Physics and Chemistry of Color*; John Wiley Sons: New York, 2001.

(29) Hassan, I.; Buseck, P. R. *Can. Mineral.* **1989**, *27*, 173.

(30) Hassan, I.; Buseck, P. R. *Am. Mineral.* **1989**, *74*, 394.

(31) Hassan, I. *Am. Mineral.* **2000**, *85*, 1383.

(32) Fechtelkord, M. *Microporous Mesoporous Mater.* **1999**, *28*, 335.

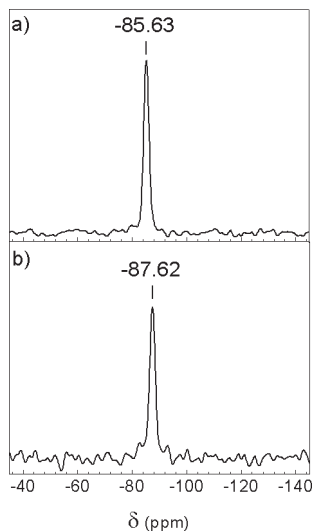


**Figure 4.**  $^{29}\text{Si}$  MAS NMR spectra of the nitrite sodalite precursor (a) and the obtained blue ultramarine-type analog (b).

analog. In both cases, just one signal is presented at  $-85.63$  ppm and  $-87.62$  ppm, respectively. These chemical shifts are close to that expected for a single chemical environment,  $\text{Q}^4(4\text{Al})$ , in synthetic sodalites with the ratio  $\text{Si}/\text{Al}$  equal to 1.<sup>25,32–34</sup> Therefore, this fact indicates the presence of one chemical environment where each Si atom is linked, through oxygen atoms, to four Al atoms within the zeolitic framework for the nitrite sodalite and obtained blue ultramarine-type analog. As stated earlier, the framework cations,  $\text{Al}^{3+}$  and  $\text{Si}^{4+}$ , remain fully ordered in the transformation process from the precursor to the blue ultramarine-type analog despite the high-temperature synthesis. Then, we conclude that the  $\text{Si}/\text{Al}$  ratio remains equal to 1. This fact contrasts with the reported ratio for the ultramarine pigments directly synthesized from metakaolin, where up to five different chemical environments,  $\text{Q}^4(4\text{Al})$ ,  $\text{Q}^4(3\text{Al})$ ,  $\text{Q}^4(2\text{Al})$ ,  $\text{Q}^4(1\text{Al})$ , and  $\text{Q}^4(0\text{Al})$ , with chemical shifts of  $-87.5$ ,  $-92.5$ ,  $-97.6$ ,  $-103.4$ , and  $-108.2$  ppm,<sup>11,14</sup> respectively, for Si atoms have been found. Thus, the  $\text{Si}/\text{Al}$  ratio is always greater than one for ultramarines obtained from metakaolin. On the other hand, there is no broadening of the signal for the obtained blue ultramarine-type analog, which could indicate that the amount of paramagnetic anion radicals  $\text{S}_2^-$  and  $\text{S}_3^-$  present is very low. The latter also contrasts with the strong broadening effect observed in dark blue ultramarines, which present a high content of paramagnetic species.<sup>11,14</sup>

The invariability of the framework ( $\text{Si}/\text{Al} = 1$ ) as well as the observed  $\beta$  cage cluster ordering at the unit cell level ( $P23$ ) for the obtained blue ultramarine-type analog indicate that the transformation process consists of the intracage transformation of the nitrite anion, the removal of the resulting species, and the diffusion of the chromophores and other species into the  $\beta$  cages. To test this hypothesis, IR spectroscopy was used. The IR spectrum of the precursor, see Figure 5a, shows a strong single band corresponding to the  $\nu_3$  mode of vibration of the entrapped  $\text{NO}_2^-$  anions

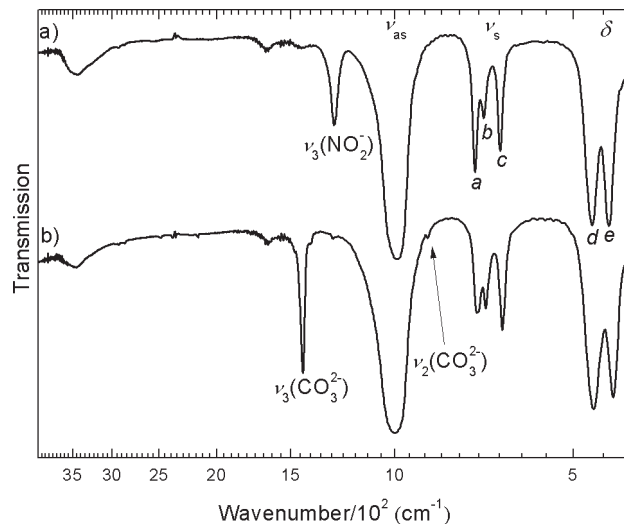


**Figure 5.** IR spectra of the nitrite sodalite precursor (a) and the obtained blue ultramarine-type analog (b).

within the  $\beta$  cages at  $1267\text{ cm}^{-1}$ ,<sup>35</sup> while the obtained blue ultramarine-type analog's IR spectrum, see Figure 5b, shows the bands assigned to the  $\nu_3(E')$  and  $\nu_2(A_2'')$  modes of the entrapped  $\text{CO}_3^{2-}$  anions at  $1430$  and  $880\text{ cm}^{-1}$ .<sup>25,32</sup> In both the precursor and the obtained blue ultramarine-type analog, the wide band at  $3500\text{ cm}^{-1}$  together with the band at  $1650\text{ cm}^{-1}$  reveal the presence of moisture and trapped water. The remaining absorption bands in the range of  $1200\text{--}400\text{ cm}^{-1}$  are mainly related to the sodalite framework.<sup>36</sup> Thus, the band in the range  $1050\text{--}950\text{ cm}^{-1}$  corresponds to the Si–O–Al asymmetric stretching ( $\nu_a$ ) mode. The three ( $a$ ,  $b$ , and  $c$ ) bands in the range  $734\text{--}657\text{ cm}^{-1}$  correspond to the Si–O–Al symmetric stretching ( $\nu_s$ ) mode, and the two ( $d$  and  $e$ ) bands at about  $465\text{--}427\text{ cm}^{-1}$  correspond to the bending ( $\delta$ ) mode. The wavenumber of the band corresponding to the  $\nu_a$  mode increases from the precursor to the obtained blue ultramarine-type analog, while the wavenumber of the bands corresponding to the  $\nu_s$  and  $\delta$  modes decrease. The absorbances of the bands corresponding to the  $\nu_s(a)$  and  $\delta(e)$  modes decrease as well. These facts agree with the slight increase of the unit cell parameter from the precursor to the blue ultramarine-type analog observed by X-ray powder diffraction and are justified by the removal of  $\text{NO}_2^-$  anions and diffusion of  $\text{CO}_3^{2-}$  anions and chromophores inside of  $\beta$  cages. It is worth noting that the absorbance of the band near  $730\text{ cm}^{-1}$  ( $\nu_s(a)$ ) is related to the degree of nonplanarity of the four-ring windows of the  $\beta$  cages and therefore to the Si–O–Al angles. Thus, the observed broadening of this band in the obtained blue ultramarine-type analog implies the presence of two different framework Si–O–Al angles, as can be observed in Figure 5. This fact agrees with the use of the space group  $P23$  to describe this structure, which presents two independent sets of 12-fold sites for the framework oxygen atoms.

Figure 6 shows the Raman spectrum of the obtained blue ultramarine-type analog where the characteristic  $\nu(590\text{ cm}^{-1})$  and  $\nu_1(550\text{ cm}^{-1})$  Raman bands of yellow  $\text{S}_2^-$  and blue ( $\text{C}_{2v}$ )  $\text{S}_3^-$  chromophores, respectively, and the  $\nu_1(A_1')$

(33) Sieger, P.; Schneider, A. M.; Wiebcke, M.; Behrens, P.; Felsche, J.; Engelhardt, G. *Chem. Mater.* **1995**, *7*, 163.

(34) Weller, M. T.; Wong, G. *J. Chem. Soc., Chem. Commun.* **1988**, *16*, 1103.

(35) Bachmann, S.; Buhl, J.-Ch. *Microporous Mesoporous Mater.* **1999**, *28*, 35.

(36) Henderson, C. M. B.; Taylor, D. *Spectrochim. Acta* **1977**, *33A*, 283.

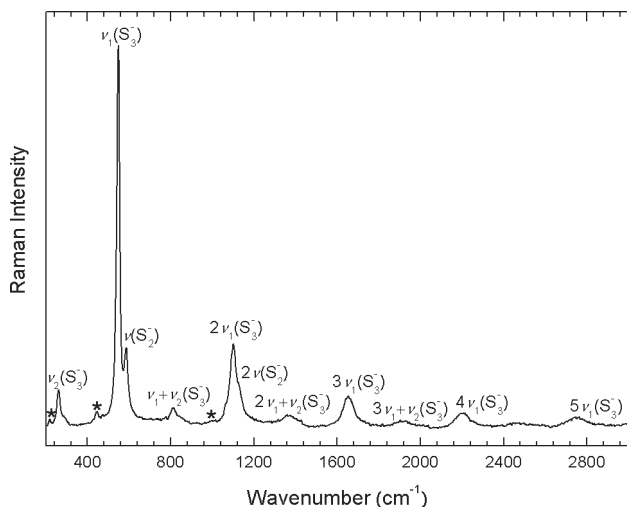


**Figure 6.** Raman spectrum of the obtained blue ultramarine-type analog. Asterisks indicate the Raman  $A_1$  bands of the framework at 240, 450, and  $980\text{ cm}^{-1}$ .<sup>34</sup>

( $1080\text{ cm}^{-1}$ ) band corresponding to the  $\text{CO}_3^{2-}$  anions are clearly observed. However, the bands corresponding to the red chromophore are not present. This feature contrasts with the Raman spectra reported for ultramarine pigments directly synthesized from metakaolin in which Raman bands corresponding to the red chromophores are observed.<sup>7</sup> The Raman data once again confirm that  $\text{NO}_2^-$  anions have been exchanged by  $\text{CO}_3^{2-}$  anions, yellow and blue chromophores.

The colorimetric parameters  $L^*$  (lightness),  $C^*$  (chroma), and  $h$  (hue) for the obtained blue ultramarine-type analog (67.87, 18.41, and 234.01) and those corresponding to a commercial reddish-blue ultramarine (77.9, 22.74, and 276.56) have been obtained from the respective diffuse reflectance spectra treated with the Kubelka–Munk function,<sup>28</sup> where bands at approximately 400 and 600 nm are assigned to yellow  $\text{S}_2^-$  ( ${}^2\Pi_{1/2u} \leftarrow {}^2\Pi_{3/2g}$ ) and blue ( $\text{C}_{2v}$ )  $\text{S}_3^-$  ( ${}^2B_1 \leftarrow {}^2A_1$ ) chromophores, see Figure 7a. It is worth noting that the average particle size of the reddish-blue standard and that of the obtained greenish-blue analog are similar (1–2  $\mu\text{m}$ ). The reflectance spectrum of the obtained ultramarine analog, just like the corresponding Raman spectrum, does not show the presence of the red chromophore. However, the spectrum of the reddish-blue ultramarine shows the absorptions at about 530 and 625 nm corresponding to the cis and trans isomers of the red chromophore  $\text{S}_4$ ,<sup>13</sup> respectively, along with the absorption of yellow and blue chromophores. The obtained colorimetric parameters are depicted in a polar plot in Figure 7b. The lightness and chroma parameters appear not to vary, while the hue does vary, making it the key parameter for these materials. The obtained blue ultramarine shows a significantly lower hue parameter than the commercial reddish one. This fact indicates the absence of red chromophores and the increase of the yellow chromophores' concentration with respect to the commercial reddish ultramarine obtained from metakaolin. This may be explained by considering the employed synthesis method. If metakaolin is used as the precursor in a typical industrial process, the sodalite framework is built up during the synthesis process, trapping the available chromophores, and for this reason, the red chromophores are entrapped together with a high amount of blue

chromophores. The insertion of the chromophores could also occur after framework formation by diffusion into the  $\beta$  cages, although it remains unclear.<sup>10</sup> However, in the obtained blue ultramarine, the nitrite sodalite precursor's framework remains, and therefore only the chromophores showing a similar kinetic diameter to that of the cavity windows can diffuse and be entrapped inside of  $\beta$  cages.

The total concentration of paramagnetic yellow  $\text{S}_2^-$  and blue  $\text{S}_3^-$  chromophores has been determined from magnetic susceptibility data as an alternative to a quantitative electron paramagnetic resonance (EPR) study. The temperature dependence of the magnetic susceptibility, previously corrected for diamagnetism, and the inverse of magnetic susceptibility for the obtained blue ultramarine-type analog reveal that there are no interactions between neighboring magnetic moments of the chromophores, and therefore the material behaves as a paramagnet, see Figure 8. From the Curie–Weiss law dependence of magnetic susceptibility, the experimental Curie constant ( $C_{\text{exp}} = 0.1202(2)\text{ emuK/mol}$ ) was determined and related to the theoretical one obtained from EPR data ( $g_{\text{iso}} = 2.030$ )<sup>9</sup> by means of the following equation:

$$C_{\text{theor}} = \frac{g^2 \times S(S+1)}{8} \quad (1)$$

The experimental/theoretical Curie constant ratio allows us to determine that around 15% of the  $\beta$  cages are occupied by chromophores. This is a rough estimate because the calculation of the theoretical Curie constant only takes the  $g$  factor corresponding to the  $\text{S}_3^-$  chromophore into account. However, despite the fact that yellow chromophores  $\text{S}_2^-$  ( $g_{\text{iso}} = 2.298$ )<sup>9</sup> are presented together with the blue  $\text{S}_3^-$  chromophores, these latter represent the majority of the chromophores, as is obvious by the sample's blue color; then, the miscalculation of the theoretical Curie constant is insignificant.

The thermal analyses curves of the obtained blue ultramarine-type analog reveal its as-expected thermal stability.<sup>22,37</sup> The initial observed weight loss from 320 to 750 K corresponds to the dehydration of the ultramarine-type analog. First, moisture is lost up to 400 K, and second, until 750 K, the absorbed water molecules (approximately 1.5 water molecules per formula unit) are released from the material. In the temperature range of 750–1400 K, the decomposition and liberation of the entrapped carbonate and chromophore anions are accompanied by the collapse of the sodalite framework to condensed aluminosilicates such as nepheline  $\text{NaAlSiO}_4$ .

Keeping the framework cations' ordering, the cage clusters' ordering, and the presence of the carbonate and chromophores anions inside of  $\beta$  cages in mind, the crystal structure of the obtained blue ultramarine-type analog was refined using powder neutron diffraction data. The used experimental data were collected on diffractometer D2B at 298 K, although a few previous measurements were performed on diffractometer D1A ( $\lambda = 1.911\text{ \AA}$ ) at 5 and 100 K at the ILL in Grenoble. After the comparison of the data, those corresponding to D2B at room temperature were selected for the crystal structure refinement as opposed to the D1A data at low temperatures. Although this data selection is unusual for a zeolite crystal structure refinement,

(37) Buhl, J.-Ch. *Thermochim. Acta* **1993**, *219*, 205.

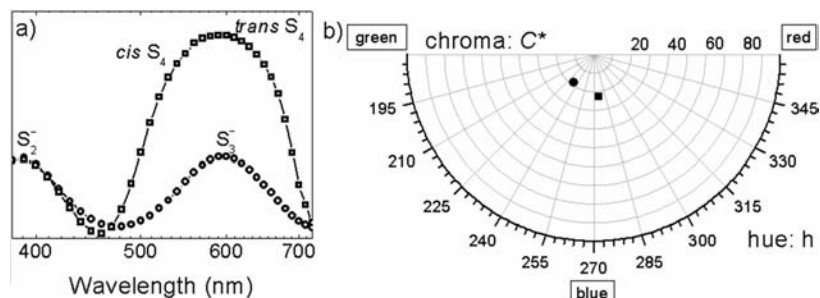


**Figure 7.** Visible diffuse reflectance spectra (a) of the obtained blue ultramarine-type analog (O) and the commercial reddish-blue ultramarine (□). The polar plot (b) shows the corresponding colorimetric parameters  $C^*$  and  $h$ .

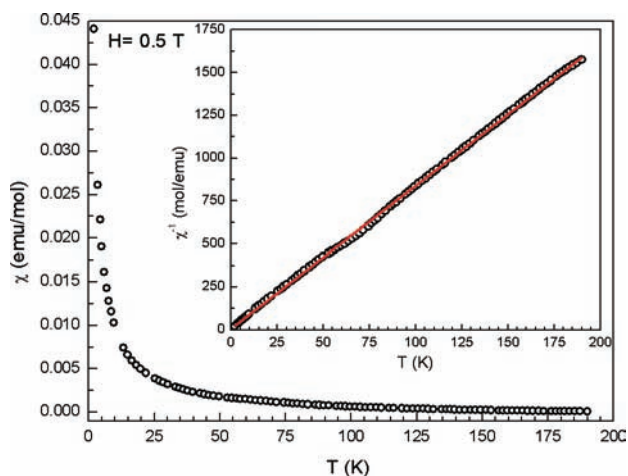


**Figure 8.** Thermal evolution of the magnetic susceptibility for the obtained blue ultramarine-type analog. The inset shows the temperature dependence of the inverse magnetic susceptibility.

the procedure is fully justified because, instead of having more thermal disorder, the carbonate and chromophore anions have a higher positional disorder due to its low symmetry in comparison to the symmetry of the  $\beta$  cages. Therefore, low-temperature data do not make structure refinement any easier. The crystallographic data and a Rietveld plot of the obtained blue ultramarine-type analog are given in Table 1 and Figure 9, respectively. The atomic positions of the hydrated carbonate nosean (space group  $P23$ )<sup>32</sup> have been used as the starting structural model, introducing the presence of chromophore groups (ca. 15% of the  $\beta$  cages) and water molecules (ca. 18% of the  $\beta$  cages). To simplify the question of the chromophores' disorder, only the blue chromophores were considered since they present the majority of chromophores. It has been reported previously that chromophore groups are 6-fold disordered, forming a regular statistical octahedron placed near the  $\beta$  cage center.<sup>3,14</sup> Thus, the three sulfur atoms of the blue chromophore were treated as a single sulfide atom located on two independent sets of 6-fold sites such as the  $6f(x,0,0)$  and  $6i(x,1/2,1/2)$  sites. For the water molecules, the atomic positions determined for nonbasic hydrosodalite were used.<sup>38,39</sup> The water oxygen atoms were placed on  $4e(x,x,x)$  positions, giving rise to a tetrahedral configuration with the water hydrogen atoms statistically distributed on  $12j(x,y,z)$  sites, interacting via hydrogen bonds with the framework oxygen

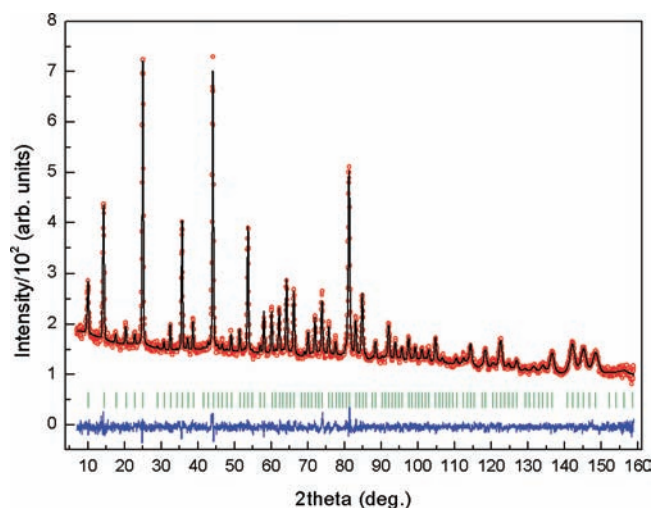


**Figure 9.** Observed (open circles), calculated (full line), and difference (lower full line) neutron powder profiles of the obtained blue ultramarine-type analog at 298 K. The row of tick marks corresponds to the Bragg positions.

**Table 1.** Crystallographic Data, Experimental Conditions, and Agreement Factors for the Crystal Structure Refinement of the Obtained Ultramarine-Type Analog

$\text{Na}_{7.88}[\text{Si}_6\text{Al}_6\text{O}_{24}](\text{CO}_3)_{0.73}(\text{S}_3)_{0.30} \cdot 1.32\text{H}_2\text{O}$	
space group	$P23$ (No. 195)
formula units/cell, $Z$	1
Molecular weight (g/mol)	986.427
cell parameter, $a$ (Å)	8.9973(1)
cell volume, $V$ (Å <sup>3</sup> )	728.35
density, $\rho$ (g/cm <sup>3</sup> )	2.249
$2\theta$ range (deg.)	6.0–160.0
step size (deg)	0.05
number of data points	3039
number of reflections	302
number of refined parameters	31
agreement factors	
$R_{\text{wp}}$	0.0334
$R_{\text{p}}$	0.0268
$R_{\text{I}}$	0.0274
$R_{\text{F}}$	0.0283
$d$	1.6

atoms. Final atomic parameters are listed in Table 2. To achieve the best results for the refinement of the sulfur atoms of the chromophore groups, the carbon and oxygen atoms of the carbonate anions and the hydrogen and oxygen atoms of the water molecules were added, with the connectivity slackly constrained by setting the C–O3, S1–S1 (or S2–S2), and H1–O4 (or H2–O4) distances equal to 1.282, 2.050, and 1.085 Å, respectively. Isotropic displacement parameters

(38) Felsche, J.; Luger, S.; Fischer, P. *Acta Crystallogr.* **1987**, *C43*, 809.

(39) Shannon, S. R.; Metiu, H. *J. Phys. Chem.* **2001**, *B105*, 3813.

**Table 2.** Atomic Parameters of the Obtained Ultramarine-Type Analog

atom	<i>P23</i>	occupancy	<i>x</i>	<i>y</i>	<i>z</i>	<i>U</i> <sub>iso</sub> (Å <sup>2</sup> )
Si	6 <i>g</i>	1	0.24479(14)	0	0.5	0.00267(10)
Al	6 <i>h</i>	1	0.25381(14)	0.5	0	0.00267
O1	12 <i>j</i>	1	0.1479(4)	0.1463(4)	0.4527(4)	0.0131(3)
O2	12 <i>j</i>	1	0.6403(4)	0.6538(4)	0.9484(4)	0.0131
Na1	4 <i>e</i>	0.9845(2)	0.1876(8)	0.1876	0.1876	0.022(4)
Na2	4 <i>e</i>	0.3147(2)	0.665(2)	0.665	0.665	0.025(5)
Na3	4 <i>e</i>	0.6703(2)	0.7768(10)	0.7768	0.7768	0.025
C	1 <i>a</i>	0.73(2)	0	0	0	0.028(4)
O3	12 <i>j</i>	0.182(2)	0.06062(8)	0.93882(7)	0.11333(2)	0.008(5)
S1	6 <i>f</i>	0.061	0.1566(6)	0	0	0.026(4)
S2	6 <i>i</i>	0.061	0.3199(4)	0.5	0.5	0.026
O4	4 <i>e</i>	0.330	0.38386(8)	0.38386	0.38386	0.026(4)
H1	12 <i>j</i>	0.110	0.29187(8)	0.38556(8)	0.30387(8)	0.18(6)
H2	12 <i>j</i>	0.110	0.37986(8)	0.4478(2)	0.28217(7)	0.18

**Table 3.** Selected Interatomic Distances (Å) and Angles (deg) of the Obtained Ultramarine-Type Analog

Framework			
Si–O1 (2×)	1.635(3)	O1–Si–O1 (1×)	115.6(4)
Si–O2 (2×)	1.625(4)	O2–Si–O2 (1×)	111.7(3)
		O1–Si–O2 (2×)	109.1(3)
		O1–Si–O2 (2×)	105.8(3)
Al–O1 (2×)	1.699(3)	O1–Al–O1 (1×)	110.6(3)
Al–O2 (2×)	1.743(4)	O2–Al–O2 (1×)	113.7(3)
		O1–Al–O2 (2×)	107.5(3)
		O1–Al–O2 (2×)	109.7(2)
Al–O1–Si	144.2(2)	Al–O2–Si	142.6(2)
Sodium Coordination			
Na1–O1 (3×)	2.440(8)	Na1–O2 (3×)	3.011(8)
Na1–O3	2.600(7)	Na1–O3	2.594(7)
Na1–S1	2.403(7)		
Na2–O1 (3×)	3.060(18)	Na2–O2 (3×)	2.561(18)
Na2–S2	2.104(18)		
Na3–O1 (3×)	3.073(10)	Na3–O2 (3×)	2.262(9)
Na3–O3	2.290(8)		
Oligosulfide Chromophore			
S1–S1	1.993(5)	S2–S2	2.292(4)
Carbonate Anion			
C–O3	1.2807(6)	O3–C–O3	119.88(8)
Water Molecule			
H1–O1	2.012(4)	H1–O4	1.0969(10)
H2–O1	2.424(4)	H2–O4	1.0814(13)
H1–O4–H2	113.04(9)		

were also constrained in the following way: Si=Al, O1=O2, Na2=Na3, S1=S2, and H1=H2. Furthermore, the occupancy factors of the sites corresponding to the chromophore groups and water molecules were fixed taking into account the data obtained from the magnetic measurements and TGA analysis, respectively. Selected interatomic distances and angles are listed in Table 3.

What becomes clear from the structure refinement in the space group *P23* is that (i) the framework is strictly composed of alternating SiO<sub>4</sub> and AlO<sub>4</sub> corner-sharing tetrahedra with the expected geometries, (ii) about 85% of the β cages are occupied following the [Na(1,3)<sub>5</sub>CO(3)<sub>3</sub>]<sup>3+</sup>:[Na(2)<sub>3</sub>]<sup>3+</sup> filling sequence to maintain the electroneutrality (Figure 10a), and (iii) the remaining 15% are filled with the sequence [Na(1)<sub>4</sub>S(1)<sub>3</sub>]<sup>3+</sup>:[Na(2,3)<sub>4</sub>S(2)<sub>3</sub>]<sup>3+</sup> (Figure 10b). Moreover, about 30% of the β cages filled by [Na(2)<sub>3</sub>]<sup>3+</sup> clusters also contain water molecules, giving rise to the fourth kind of

clusters, [Na(2)<sub>3</sub>H(1,2)<sub>2</sub>O(4)]<sup>3+</sup>. Thus, the carbonate anions are coordinated by four Na1 (2.600(7), 2.594(7) Å) cations and by one Na3 (2.290(8), 3.748(8) Å) cation to locally balance the charge. The S1 chromophores are coordinated by four Na1 (2.403(7) Å) cations, while S2 chromophores probably interact with four Na2 (2.104(18), 3.748(18) Å) or Na3 (3.628(8) Å) cations. It is surprising that the observed Na3–O3 and Na2,3–S2 distances are either too short or too long. However, it can be explained by accounting for a fast dynamical exchange between Na2 and Na3 sites (Figure 10b) and the orientational disorder of the carbonate and chromophore anions, which has been previously reported.<sup>33</sup> On the other hand, the water oxygen atoms O4 are located about 2.11 Å from the plane of the six-ring windows and the corresponding hydrogen atoms interacting via hydrogen bonds with two framework oxygen atoms, <H1,H2–O1> = 2.20 Å. Finally, the isotropic temperature factors of the

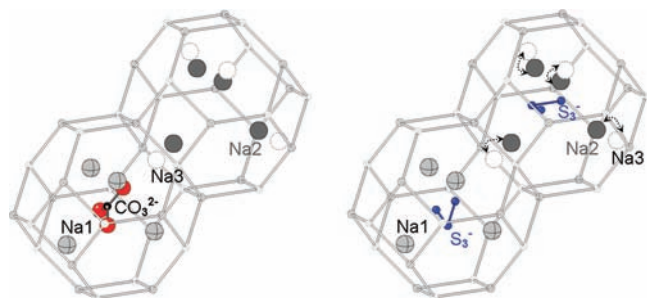


**Figure 10.**  $\beta$  cage  $[\text{Na}_5\text{CO}_3]^{3+}:[\text{Na}_3]^{3+}$  (left) and  $[\text{Na}_4\text{S}_3]^{3+}:[\text{Na}_4\text{S}_3]^{3+}$  (right) filling sequences in the obtained blue ultramarine-type analog. The black double arrow shows the dynamic exchange between Na2 and Na3 sites.

carbonate and chromophore anions demonstrate the large positional disorder, as is expected. The isotropic temperature factor of C is higher than that of oxygen O3 because of the off-center position.

These results reveal that the obtained blue ultramarine-type analog can be considered as a solid solution with different cage fillings. Therefore, our previous spectroscopic and magnetic studies have been essential to achieving the partial structure solution of this material using neutron powder diffraction data.

## Conclusions

A new synthetic route for ultramarine analogs has been reported using nitrite sodalite as the starting material. X-ray and neutron powder diffraction, SAED, IR, and Raman studies together with colorimetric, magnetic, and thermal analyses show that ultramarine-type materials can be obtained from nitrite sodalites with a chromophore concentration of about 0.30 mol per formula unit, which is enough to have blue ultramarines with a green shade. This is a new kind of ultramarine analog in which yellow and blue chromophores are entrapped together with carbonate anions within  $\beta$  cages. The shown average filling indicates the lowest symmetry ( $P2_3$ ) for a cubic ultramarine analog. Therefore, the use of nitrite sodalite as a precursor allows us to obtain greenish-blue ultramarines, removing the red shade of the analog by the selective trapping that takes place through sodalite cavity windows where the diffusion of large red chromophores into the  $\beta$  cages is unallowed.

**Acknowledgment.** The authors thank the Nubiola Inorganic Pigments Company and the Spanish MCI (Research Project MAT2007-63497) for financial support. We also thank ILL for the beamtime allocation through the EASY access system (<http://www.ill.eu/users/applying-for-beamtime/easy-easy-access-system>).